Available online at www.sciencedirect.com
ScienceDirect
Chemical Physics Letters 451 (2008) 293–300
CHEMICAL PHYSICS LETTERS
www.elsevier.com/locate/cplett

A non-equilibrium multiscale simulation paradigm

Shaofan Li *, Ni Sheng, Xiaohu Liu

Department of Civil and Environmental Engineering, University of California, 783 Davis Hall, Berkeley, CA 94720, USA

Received 23 October 2007; in final form 30 November 2007
Available online 8 December 2007

Abstract

A con-current multiscale non-equilibrium molecular dynamics is proposed. The notion of *multiscale canonical element ensemble* is put forth, which enables us to employ the coarse grain field as a heat bath, and it is accomplished by using a *distributed Nośe–Hoover thermostat network*. In doing so, it guarantees that the non-equilibrium molecular dynamics returns to a canonical equilibrium state when external disturbances vanish, which may have not been the case for the non-equilibrium molecular dynamics in the literature. We have shown that the non-equilibrium distribution function is canonical.

1. Introduction

The non-equilibrium thermal–mechanical process at small scales, for instance nanoscale heat transfer, in which the length and/or time scales span from the molecular to the continuum, is a subject of increasing importance to energy conversion, biotechnology, microelectronics, biochemical detection, and material synthesis and failure analysis. The capacity to simulate thermal–mechanical couplings in non-equilibrium states at small scales are vital to the understanding of transport mechanisms of energy conversion and to the advancement of reliability of micro and nano-electronics.

The conventional molecular dynamics (MD) is a dynamics of the micro-canonical ensemble, and it is unable to provide statistical characters to the physics problem that it simulates. To extrapolate statistical thermodynamics information from molecular dynamics simulations, the simulations of equilibrium ensemble molecular dynamics (EEMD) are required at a fixed temperature or fixed pressure or specified chemical potentials. Various EEMDs have been implemented by using different thermostats, e.g. [1–5]. However, the EEMD is unable to simulate problems with spatial or temporal temperature gradients.

Since early 1980s, the non-equilibrium molecular dynamics (NEMD) has become a major simulation tool for simulations of non-equilibrium processes. The NEMD has been used to compute transport coefficients [6–8] and to simulate viscous flows [9–11] and plastic deformations [12]. In the literatures, there are mainly three types of NEMDs:

(1) Prescribed-flow-driven NEMD
(2) The synthetic NEMD, and
(3) Boundary-flux-driven NEMD

The representatives of the first type NEMDs are the well-known DOLLS and SLLOD algorithms, e.g. [9–11,13–16], in which the MD system is driven out of equilibrium by prescribed constant flow field. To the best of the authors' knowledge, this type of NEMDs are only used in special cases such as simulation of the Couette flows for extrapolating the viscous coefficient. In the second type of NEMDs [7,14,17–19], an artificial external field is prescribed to drive the system out of equilibrium, however, the artificial external field is judicially chosen such that it renders the phase–space flux divergence-free, or it enforces the so-called *adiabatic incompressibility condition* (AIΓ) [14]. The synthetic NEMD is related to the Green–Kubo linear response theory, and it has been mainly used to extrapolate the transport coefficients of non-equilibrium states from an

* Corresponding author. Fax: +1 510 642 8928.
E-mail address: shaofanli@gmail.com (S. Li).

0009-2614/$ - see front matter © 2007 Elsevier B.V. All rights reserved.
doi:10.1016/j.cplett.2007.11.099

equilibrium state simulation, which is usually not used as a direct non-equilibrium multiscale simulation.

Although both the first and second types of NEMDs have firm statistical physics foundation, they are not intended as the direct simulation tools. The third type of NEMDs are the most popular NEMDs used in practice, and it has been the workhorse in performing direct atomistic or molecular simulations, and it has been extensively used in the field of heat transfer and thermal engineering, e.g. [20–24], among many others. In this type of NEMDs, the system is driven out of equilibrium by prescribed boundary heat fluxes, which are either heat sources or heat sinks, and they are enforced by either thermostat or velocity scaling techniques.

A main shortcoming of the this type of NEMDs is: when the boundary heat flux is absent, the system cannot automatically return to a thermodynamic equilibrium state, instead it becomes a micro-canonical ensemble molecular dynamics system. In the literature, many researchers automatically assumed that phonons in such system are bosons that obey the Bose–Einstein distribution. In fact, it has been quite popular that the phonon distributions obtained in such simulations are being used to extrapolate transport coefficients.

In recent years, several multiscale methods have been proposed to solve nanoscale thermal–mechanical problems, and they have been successful for certain problems, for examples, Abraham and his co-workers' macroscopic, atomistic, *ab initio* dynamics (MAAD) [25], Rudd and Broughton's coarse-grained molecular dynamics (CGMD) [26,27], Liu and his co-workers' bridging scale method [28,29], E and his co-workers' heterogeneous multiscale method [30,31], and others.

In this Letter, we report a novel multiscale non-equilibrium molecular dynamics (MS-NEMD) method that provides a NEMD simulation capable of spontaneously and automatically returning or reaching to an equilibrium state when external disturbances are absent, and it generalizes the NEMD to the setting of con-current multiscale simulations that can simulate nano-scale thermal–mechanical interactions of realistic size.

2. Formulations

We start with the multiscale decomposition proposed in [28,32], which decomposes the discrete atomistic displacement field, $\mathbf{q}$, into a coarse scale part and a fine scale part: $\mathbf{q} = \bar{\mathbf{q}} + \mathbf{q}'$. The symbol $\bar{}$ indicates coarse scale quantities, and the symbol $'$ indicates the fine scale quantities. We assume that the coarse scale atomistic displacements can be described by a continuous mean field, $\bar{\mathbf{u}}(\mathbf{X})$, which can be represented by a finite element (FE) interpolation field

$$\bar{\mathbf{u}} = \mathbf{N}(\mathbf{X})\mathbf{d} \quad \Rightarrow \quad \bar{\mathbf{q}} = \mathbf{N}(\mathbf{X}_a)\mathbf{d} \tag{1}$$

where $\mathbf{X}$ denotes the spatial position vector, $\mathbf{X}_a$ are the spatial positions of atoms, $\mathbf{d}$ is the FE nodal displacement array, and $\mathbf{N}(\mathbf{X})$ is the matrix of FE interpolation functions, or shape functions evaluated at $\mathbf{X}$. It is assumed that atoms or molecules are moving in a continuous ambient space. In one-dimensional case, the linear FE shape function $\mathbf{N}(\mathbf{X}) = \{N_i(X)\}_{i=1}^{n_{\text{node}}}$ can be expressed as:

$$N_i(X) = \begin{cases} \frac{X - X_{i-1}}{X_i - X_{i-1}} & \text{if } X \in [X_{i-1}, X_i] \\ \frac{X_{i+1} - X}{X_{i+1} - X_i} & \text{if } X \in [X_i, X_{i+1}] \end{cases} \tag{2}$$

Here n_{node} is the number of FE nodes.

With the bridging scale formulation, both the coarse scale components and the fine scale components can be obtained from the total scale variable [28]: $\bar{\mathbf{q}} = \mathbf{P}(\mathbf{X}_a)\mathbf{q}$, $\mathbf{q}' = \mathbf{Q}(\mathbf{X}_a)\mathbf{q}$, where $\mathbf{P}$ and $\mathbf{Q}$ are projection operators defined as

$$\mathbf{P} = \mathbf{N}\mathbf{M}^{-1}\mathbf{N}^{\mathrm{T}}\mathbf{M}_a \quad \text{and} \quad \mathbf{Q} = \mathbf{I} - \mathbf{P}$$

where superscript T denotes transpose, $\mathbf{M}_a = \mathrm{diag}(m_1, m_2, \ldots, m_N)$ is the diagonal mass matrix for atoms, $\mathbf{M} := \mathbf{N}^{\mathrm{T}}\mathbf{M}_a\mathbf{N}$ is the coarse scale mass matrix, and $\mathbf{I}$ is identity matrix.

The essence of the con-current multiscale simulation is that the coarse scale motion is solved over the *entire domain* by using a coarse graining model driven by initial/boundary conditions, from which we can obtain the continuous mean field $\bar{\mathbf{u}}$; whereas fine scale fluctuations are solved via a first-principle based model for specific regions, or con-current regions, where atomistic resolution is desired. The fine scale model is seamlessly and simultaneously incorporated into the coarse scale computations by providing updated constitutive and thermodynamics information that are based on the fine scale computations. A main difference between the proposed MS-NEMD and other molecular dynamics is that in the MS-NEMD the fine scale model alone cannot provide statistics details even within the fine scale region. The fine scale molecular dynamics depends on inputs of the coarse scale mean field in different ways. First the fine scale molecular dynamics is driven out of the equilibrium by the coarse scale mean field that depends on external force field and mechanical boundary condition, and second, as we shall explain later, the amplitude of fine scale fluctuations is regulated by thermodynamic temperature, which is a macroscale quantity depending on boundary heat fluxes, interior heat sources, and coarse scale heat convection.

We first consider the adiabatic multiscale simulation in the con-current region. The multiscale displacement decomposition implies similar decompositions for the velocity and the linear momentum, i.e. $\mathbf{v} = \bar{\mathbf{v}} + \mathbf{v}'; \mathbf{p} = \bar{\mathbf{p}} + \mathbf{p}'$. This suggests the following multiscale adiabatic Hamiltonian for a single element ensemble e

$$H_e^{\text{adia}} = \sum_{i=1}^{N_e} \frac{1}{2m_i}\bar{\mathbf{p}}_i \cdot \bar{\mathbf{p}}_i + \sum_{i=1}^{N_e} \frac{1}{2m_i}\mathbf{p}'_i \cdot \mathbf{p}'_i + U(\mathbf{q}) \tag{3}$$

where N_e is the number of atoms in the element ensemble e, $\mathbf{p}_i$ and m_i are, respectively, the momentum and mass of the atom i, and $U(\mathbf{q})$ is the atomistic potential. Note that the

coarse scale momentum is orthogonal to the fine scale momentum, i.e.

$$\sum_i \bar{\mathbf{p}}_i \cdot \mathbf{p}'_i = 0 \quad \Leftarrow \quad \mathbf{PQ} = \mathbf{P}(\mathbf{I}-\mathbf{P}) \equiv 0 \tag{4}$$

The two-scale equations of motion are then given as

$$\dot{\mathbf{q}}_i = \frac{\partial H_e^{\text{adia}}}{\partial \mathbf{p}_i} = \frac{\bar{\mathbf{p}}_i}{m_i} + \frac{\mathbf{p}'_i}{m_i} \tag{5}$$

$$\dot{\mathbf{p}}_i = -\frac{\partial H_e^{\text{adia}}}{\partial \mathbf{q}_i} = -\frac{\partial U(\mathbf{q})}{\partial \mathbf{q}_i} = \mathbf{f}_i \tag{6}$$

$$\dot{\bar{\mathbf{q}}}_i = \frac{\partial H_e^{\text{adia}}}{\partial \bar{\mathbf{p}}_i} = \frac{\bar{\mathbf{p}}_i}{m_i} \tag{7}$$

$$\dot{\bar{\mathbf{p}}}_i = -\frac{\partial H_e^{\text{adia}}}{\partial \bar{\mathbf{q}}_i} = -\frac{\partial U(\mathbf{q})}{\partial \bar{\mathbf{q}}_i} = \mathbf{f}_j \frac{\partial \mathbf{q}_j}{\partial \bar{\mathbf{q}}_i} \tag{8}$$

where $\mathbf{f}_i$ is the external force acting on the atom i.

The coarse scale displacement and velocity fields are approximated by FE interpolations, i.e.

$$\bar{\mathbf{q}} = \mathbf{N}\mathbf{d}, \quad \text{and} \quad \bar{\mathbf{p}} = \mathbf{M}_{\text{a}}\mathbf{N}\dot{\mathbf{d}} \tag{9}$$

we can then deduce that

$$\begin{aligned}
\dot{\bar{\mathbf{p}}}_i &= m_i \frac{\mathrm{d}}{\mathrm{d}t}\left(\sum_J N_J(\mathbf{x}_i)\dot{\mathbf{d}}_J\right) \\
&= m_i\left(\sum_J N_J(\mathbf{x}_i)\ddot{\mathbf{d}}_J + \sum_J B_J(\mathbf{x}_i)\dot{\mathbf{d}}_J\dot{\bar{\mathbf{q}}}_i + \sum_J B_J(\mathbf{x}_i)\dot{\mathbf{d}}_J\frac{\mathbf{p}'_i}{m_i}\right) \\
&\approx \sum_J B_J(\mathbf{x}_i)\dot{\mathbf{d}}_J \cdot \mathbf{p}'_i = \frac{\partial \bar{\mathbf{v}}_i}{\partial \mathbf{x}} \cdot \mathbf{p}'_i
\end{aligned} \tag{10}$$

where $B_J(\mathbf{x}_i) = \partial N_J(\mathbf{x}_i)/\partial \mathbf{x}_i$. Note that the above expression is exact when there is no coarse scale external force, because

$$\begin{aligned}
\frac{\mathrm{d}}{\mathrm{d}t}\left(\sum_J N_J(\mathbf{x}_i)\dot{\mathbf{d}}_J\right)_{\text{coarse scale}} &= \left(\sum_J N_J(\mathbf{x}_i)\ddot{\mathbf{d}}_J \right. \\
&\left. + \sum_J B_J(\mathbf{x}_i)\dot{\mathbf{d}}_J\dot{\bar{\mathbf{q}}}_i\right) = 0
\end{aligned}$$

In this case, the MS-NEMD algorithm degenerates to a generalized DOLLS formulation.

Moreover, we note that the fine scale kinetic temperature can be determined by the fine scale momentums or the fine scale velocities – a generalization of peculiar velocities in NEMD simulations

$$\frac{3}{2}(N_e - 1)k_{\text{B}}T_e = \left\langle \sum_i \frac{\mathbf{p}'_i \cdot \mathbf{p}'_i}{2m_i} \right\rangle \tag{11}$$

where k_{B} is the Boltzmann constant, T_e is the kinetic temperature for the element ensemble e, and $\langle\cdot\rangle$ denotes averaging in time. Note that at the end of each fine scale time integration cycle, we use the kinetic temperature T_e to update the temperature at the FE node e [33]. The instantaneous kinetic temperature T_{ins} is defined as

$$\frac{3n(\mathbf{x},t)k_{\text{B}}T_{\text{ins}}(\mathbf{x},t)}{2} = \sum_i \frac{\mathbf{p}'_i \cdot \mathbf{p}'_i}{2m_i}\delta(\mathbf{x}_i - \mathbf{x})$$

where $\delta(\mathbf{x}_i - \mathbf{x})$ is the Dirac delta function, and $n(\mathbf{x},t)$ is defined as the instantaneous local particle number density.

To couple the local equilibrium state with the coarse scale heat conduction, we introduce a local Nosé–Hoover thermostat in each element ensemble such that the fine scale equations of motion become

$$\begin{aligned}
&\dot{\mathbf{q}}_i = \frac{\bar{\mathbf{p}}_i}{m_i} + \frac{\mathbf{p}'_i}{m_i}, \quad \dot{\mathbf{p}}'_i = \mathbf{f}_i - \dot{\bar{\mathbf{p}}}_i - \xi_e\mathbf{p}'_i, \quad \forall i \in \mathbf{N}_e, \\
&\mathbf{N}_e = \{1, \ldots, N_e\}
\end{aligned} \tag{12}$$

and

$$\dot{\xi}_e = \frac{1}{Q_e}\left(\sum_{i\in\mathbf{N}_e}\frac{\mathbf{p}'_i \cdot \mathbf{p}'_i}{2m_i} - 3N_e k_{\text{B}}T_e\right) \tag{13}$$

where ξ_e is an auxiliary variable and Q_e is its pseudo mass, and the temperature T_e for each element ensemble is the coarse scale FEM nodal temperature at node e. The main novelty of the present multiscale formulation is the use of the Nośe–Hoover thermostat network defined in (12), (13), which is illustrated in Fig. 1. One may compare this with the canonical ensemble equilibrium MD [1,2], in which the temperature is a constant. In the MS-NEMD, the coarse scale temperature distribution is non-uniform and evolving with time, the FE nodal temperature changes from node to node and time to time. Therefore, the thermodynamics temperature varies among different element ensembles and from different coarse scale time steps.

The conventional Nośe–Hoover thermostat renders the molecular dynamics system a canonical ensemble. Will the proposed Nośe–Hoover thermostat network provide a similar role in the non-equilibrium simulation? Consider

$$H_e^* = \sum_{i=1}^{N_e}\frac{\bar{\mathbf{p}}_i \cdot \bar{\mathbf{p}}_i}{2m_i} + \sum_{i=1}^{N_e}\frac{\mathbf{p}'_i \cdot \mathbf{p}'_i}{2m_i} + U_e(\mathbf{q}) + J_{e+1} - J_{e-1}$$

where J_{e+1} and J_{e-1} are boundary fluxes of the element ensemble e. It then can be shown that

$$\begin{aligned}
\frac{\mathrm{d}}{\mathrm{d}t}H_e^* - \dot{J}_{e+1} + \dot{J}_{e-1} &= \sum_i\left(\frac{1}{m_i}(\dot{\mathbf{p}}'_i \cdot \mathbf{p}'_i + \dot{\bar{\mathbf{p}}}_i \cdot \bar{\mathbf{p}}_i) - \mathbf{f}_i \cdot \dot{\mathbf{q}}_i\right) \\
&= \sum_i \frac{-1}{m_i}\left(\mathbf{p}'_i \cdot \dot{\bar{\mathbf{p}}}_i + \xi_e\mathbf{p}'_i \cdot \mathbf{p}'_i \right. \\
&\quad \left. + \bar{\mathbf{p}}_i \cdot \dot{\mathbf{p}}'_i + \xi_e\bar{\mathbf{p}}_i \cdot \mathbf{p}'_i\right) \\
&= -\xi_e\left(\sum_i \frac{1}{m_i}\mathbf{p}'_i \cdot \mathbf{p}'_i\right) \\
&\quad - \xi_e\left(\sum_i \frac{1}{m_i}\mathbf{p}'_i \cdot \bar{\mathbf{p}}_i\right) \\
&\quad - \frac{\mathrm{d}}{\mathrm{d}t}\left(\sum_i \frac{1}{m_i}\mathbf{p}'_i \cdot \bar{\mathbf{p}}_i\right)
\end{aligned}$$

By virtue of (4) and (13), we have

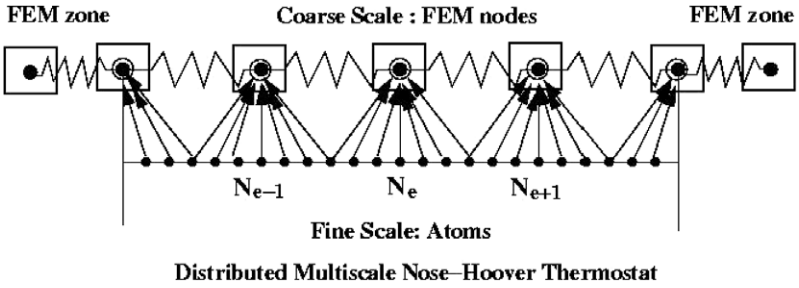

Fig. 1. The structure of distributed Nośe–Hoover thermostat network.

$$\frac{\mathrm{d}}{\mathrm{d}t}\left(H_e^* + \frac{1}{2}Q_e\xi_e^2\right) = -3N_e\xi_e k_\mathrm{B}T_e + \dot{J}_{e+1} - \dot{J}_{e-1}$$

It should be pointed out that each element ensemble is an open system with fluxes exchange among themselves. Assume that the multiscale boundary is adiabatic and inter-element fluxes cancel each other if we sum the above expression in all elements. Thus

$$\sum_{e=1}^{n_\mathrm{elem}}\left(\frac{\mathrm{d}}{\mathrm{d}t}\left(H_e^* + \frac{1}{2}Q_e\xi_e^2\right)\right) = -\sum_{e=1}^{n_\mathrm{elem}} 3N_e\xi_e k_\mathrm{B}T_e$$

where n_elem denotes the total number of element ensembles. On the other hand, the Liouville equation for distribution function in each element ensemble is

$$\frac{\mathrm{d}f_e}{\mathrm{d}t} = -f_e\sum_{i=1}^{N_e}\left(\frac{\partial\dot{\mathbf{q}}_i}{\partial\mathbf{q}_i} + \frac{\partial\dot{\mathbf{p}}_i'}{\partial\mathbf{q}_i}\right) - f_e\frac{\partial\dot{\xi}_e}{\partial\xi_e} = 3N_e\xi_e f_e$$

where f_e is the probability density distribution function. This leads to

$$\sum_{e=1}^{n_\mathrm{elem}}\left(\frac{\mathrm{d}}{\mathrm{d}t}\left(H_e^* + \frac{1}{2}Q_e\xi_e^2\right) + \frac{1}{\beta_e}\frac{\mathrm{d}}{\mathrm{d}t}\log f_e\right) = 0$$

where $\beta_e = (k_\mathrm{B}T_e)^{-1}$.

A possible solution for the distribution function in each element ensemble is

$$f_e(\mathbf{q},\mathbf{p}',\xi_e,t) = C\exp\left[-\beta_e\left(H_e^* + \frac{1}{2}Q_e\xi_e^2\right)\right] \tag{14}$$

where C is an arbitrary constant. We can then conclude that the proposed fine scale dynamics model does indeed produce a canonical non-equilibrium thermodynamics, e.g. [34,35], which is superior to the algorithm proposed early in [36]. Moreover, when external disturbances disappear, the MS-NEMD will degenerate to the Nośe–Hoover canonical ensemble MD.

The classical canonical ensemble, or NVT ensemble, is a system embedded within an infinitely large thermal reservoir, whose temperature remains constant during an equilibrium process. What is the thermal reservoir in non-equilibrium multiscale simulations? To answer this question, we propose a notion of *multiscale canonical ensemble*: We argue that the coarse scale of MS-NEMD may be served as '*the coarse scale reservoir*' within the duration of the coarse grain time scale length. This postulate may be valid because the coarse grain is defined based on the '*slow variable approximation*' and the '*Markovian approximation*' [37]. Each approximation is characterized by a specific time scale length. Therefore, the coarse scale thermodynamic temperature may be considered to be constant within duration of the coarse scale time scale, which can be chosen as the coarse scale time step in computations. The fine scale dynamics and the coarse scale dynamics can exchange thermal–mechanical information through a thermostat network (12), (13), equations of motions (5)–(8), and the multiscale decomposition (1). Figuratively, the fine scale system may be thought as saturated within the coarse scale system. During each coarse scale time step, the fine scale system may reach to a local equilibrium, so we may call each element ensemble as *a multiscale canonical ensemble system* in the sense of local equilibrium approximation (LEA). Fig. 2 compares the classical thermal reservoir with the proposed coarse scale reservisor.

Last, the coarse-grained model used in this work is based on a coarse-grained Helmholtz free energy, which is constructed by assuming the Cauchy–Born rule and the quasi-harmonic approximation [38,39]. The coarse-grained free energy function allows us to derive macroscopic coupled thermo-mechanical equations. If the local deformation is homogeneous, the total atomistic potential U_0 can be written as: $U_0 = U_0(\mathbf{F}^e)$, where $\mathbf{F}^e$ is the deformation gradient. The coarse-grained Helmholtz free energy in an element ensemble has the following form [40]:

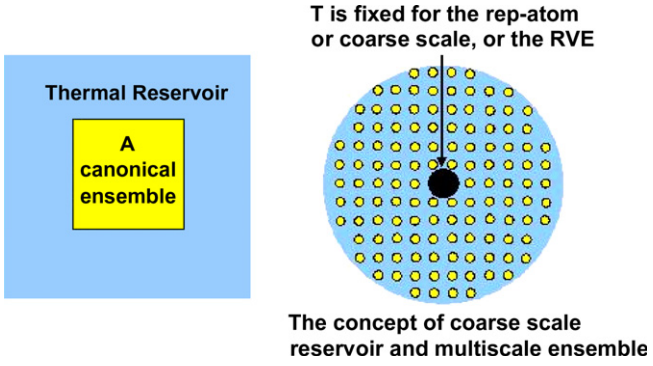

Fig. 2. The concept of multiscale canonical ensemble.

$$\mathscr{F}(\mathbf{F}^e, T_e) = U_0(\mathbf{F}^e) + k_B T_e \sum_{i=1}^{N_e} \log\left[2\sinh\left(\frac{\hbar\omega_i(\mathbf{F}^e)}{4\pi k_B T_e}\right)\right]$$

where $\hbar$ is Planck's constant divided by 2π, and ω_i are normal mode frequencies for the lattice, which can be determined via harmonic approximation. Subsequently, we can derive the expressions for the state variables such as the entropy S and the first Piola–Kirchhoff stress $\mathbf{P}$

$$S = -\frac{\partial \mathscr{F}}{\partial T_e} = \frac{k_B}{T_e}\sum_i \left(\frac{\hbar\omega_i(\mathbf{F}^e)}{4\pi k_B}\right)\coth\left(\frac{\hbar\omega_i(\mathbf{F}^e)}{4\pi k_B T_e}\right) - k_B \sum_i \log\left[2\sinh\left(\frac{\hbar\omega_i(\mathbf{F}^e)}{4\pi k_B T_e}\right)\right]$$

$$\mathbf{P}(\mathbf{F}^e, T_e) = \frac{1}{\Omega_e}\frac{\partial \mathscr{F}}{\partial \mathbf{F}^e} = \frac{1}{\Omega_e}\left\{U_0'(\mathbf{F}^e) + \frac{\hbar}{4\pi}\sum_i \left[\coth\left(\frac{\hbar\omega_i(\mathbf{F}^e)}{4\pi k_B T_e}\right)\omega_i'(\mathbf{F}^e)\right]\right\}$$

where Ω_e denotes the volume of the element ensemble e. Other transport coefficients, e.g. the specific heat at constant volume C_V and the specific heat at constant temperature $\mathbf{C}_T$ are defined as

$$C_V(\mathbf{F}^e, T_e) = -T_e\frac{\partial^2 \mathscr{F}}{\partial T^2} \quad \text{and} \quad \mathbf{C}_T(\mathbf{F}^e, T_e) = -T_e\frac{\partial^2 \mathscr{F}}{\partial T \partial \mathbf{F}^e}$$

Note that in the proposed MS-NEMD, the above transport coefficients will be later updated via the response theory by utilizing the fine scale computation results [33].

The equation of motion at coarse scale is

$$\nabla_{\mathbf{X}}\cdot\mathbf{P} + \rho_0\mathbf{B} = \rho_0\ddot{\mathbf{u}} \quad \forall \mathbf{X}\in\Omega_0 \tag{15}$$

where ρ_0 is the density in material configuration, $\mathbf{B}$ is the body force, $\nabla_{\mathbf{X}}$ is the material gradient operator in contract to ∇ as the spatial gradient operator, and Ω_0 denotes the entire coarse scale domain in the referential configuration. Consider the first law of thermodynamics

$$\dot{w} = \rho_0 z - \nabla_{\mathbf{X}}\cdot\mathbf{Q} + \mathbf{P}:\dot{\mathbf{F}},$$

where w is the internal energy per unit reference volume, z is the heat source per unit mass, and $\mathbf{Q}$ is the heat flux vector. By exploiting the Fourier law: $\mathbf{Q} = -\mathbf{K}_T\cdot\nabla T$ where $\mathbf{K}_T$ is the thermal conductivity tensor, we can write the following coupled heat conduction equation

$$\frac{\mathbf{C}_T}{\Omega_0}:\dot{\mathbf{F}} + \frac{C_V}{\Omega_0}\dot{T} = \rho_0 z + \nabla_{\mathbf{X}} J\mathbf{F}^{-1}\cdot\mathbf{K}_T\cdot\mathbf{F}^{-T}\cdot\nabla_{\mathbf{X}}T \tag{16}$$

where J is the determinant of the Jacobian. Eqs. (15) and (16) form the complete set of governing equations for the coarse grain model. A detailed coarse scale finite element formulation and time integration is presented in [33].

3. Numerical example

To demonstrate effectiveness of the MS-NEMD, we have carried out a numerical example on one-dimensional shock wave propagation. In computations, a special Frenkel–Kontorova potential, or the FPU-β potential [22,41], is used

$$U(\mathbf{q}) = \sum_i \left(\frac{k}{2}(|x_i - x_j| - a)^2 + \frac{\mathscr{K}}{2}(x_i - a\,\mathrm{int}(x_i/a))^2 - \frac{\mathscr{K}}{24}(x_i - a\,\mathrm{int}(x_i/a))^4\right), \quad |i-j| = 1. \tag{17}$$

This type of potential has been used in other multiscale simulations [30]. In the present simulation, we use the following normalized parameters: $a = 1, k = 1, \mathscr{K} = 0.7, m = 1, \tilde{k}_B = k_B t_c^2/m_c L_c^2$, and $\tilde{\hbar} = \hbar t_c/m_c L_c^2$. The characteristic mass, length and time are chosen as: $m_c = 26.98$ amu, $L_c = 3.253$ A and $t_c = 2.0\times10^{-13}$ s, respectively. A domain of [0, 1000] with 1001 atoms is considered. There are 50 fine scale FE elements and each of them consists of 20 atoms. Linear FEM shape functions are used. The coarse scale time step is 0.1 and the fine scale time step is 0.01.

In the first simulation, we use the MS-NEMD to simulate a shock wave or a dislocation propagation. A constant external force $f = 0.04$ is applied to every atom, which is slightly higher than the critical force that moves the dislocation. The critical force should be understood as the critical lattice friction, i.e. the Peierls force [42]. When the driving force is above such value, a dislocation or a strong discontinuity can move by overcoming its barrier [43,44]. The initial temperature in this example is chosen as $T_0 = 100$ K. Fig. 3 shows snapshots of displacement, instantaneous kinetic (fine scale) temperature, and thermodynamic (coarse scale) temperature profiles. One can observe extreme high temperature peak moving with the shock front, which generates coarse scale heat wave propagation. This example reveals the capacity of the MS-NEMD to simulate a non-equilibrium process with both spatial and temporal temperature gradients.

In the second simulation, a sub-critical load, $f = 0.03$, is applied along the lattice, which is initially heat up to $T_0 = 200$ K. The results of the MS-NEMD simulation are compared with that of conventional NEMD (the third type). In this case, the simulation results of the conventional NEMD predict a stationary shock wave, which does not propagate along the lattice (Fig. 4a). In the MS-NEMD simulation (Fig. 4b), under the same external load and the same initial temperature, the shock wave moves from right to left, which indicates the thermal activation of dislocation motions. Note that similar conclusions may have been drawn based on the Nośe–Hoover equilibrium MD simulation. However, in reality the shock wave is propagating in a non-equilibrium state far away from the equilibrium, in which both spatial and temporal temperature gradients are present and changing. To the best of the authors' knowledge, this is the first successful numerical simulation of thermal activation of 'dislocation' under non-equilibrium state. The fine scale calculation provides the essential source for thermal–mechanical coupling at both scales, and the activation of dislocation is clearly due to

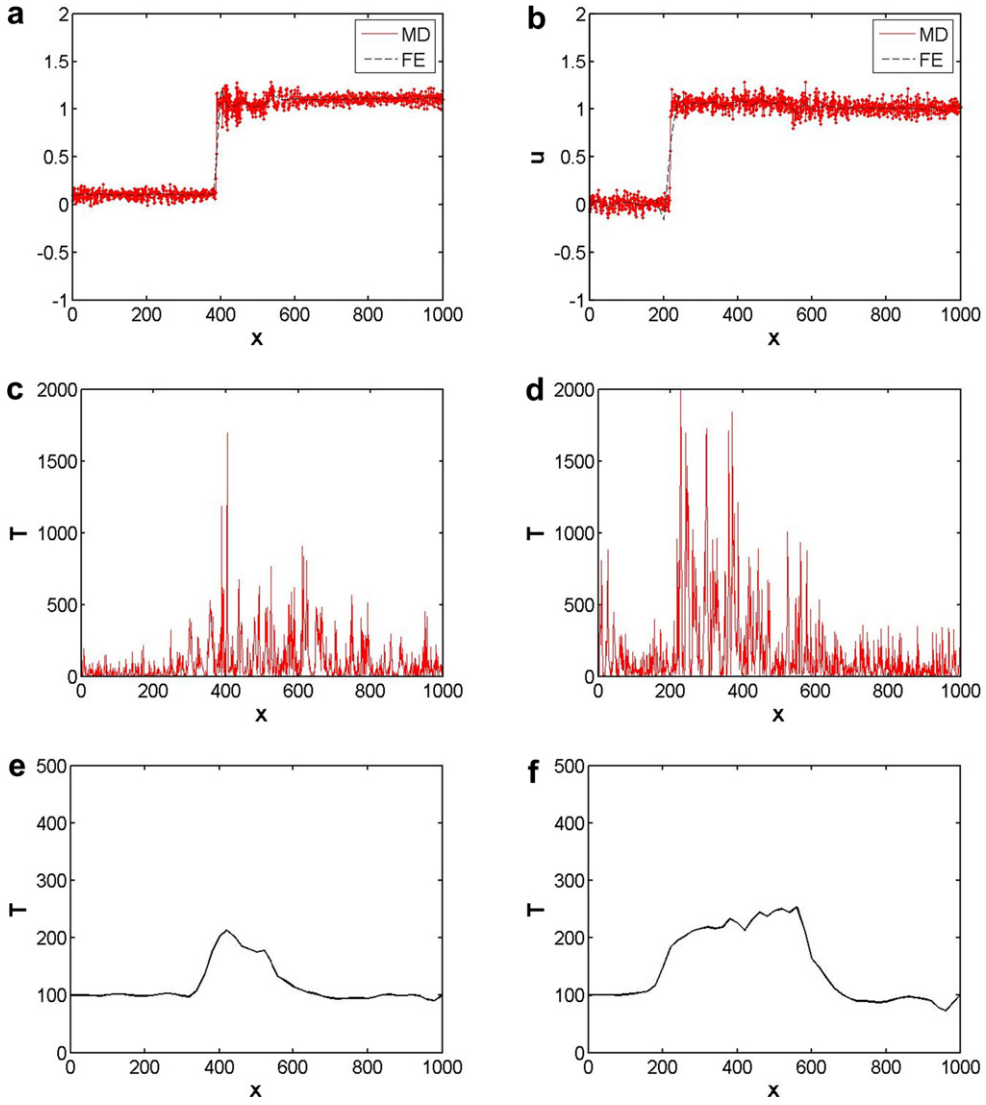

Fig. 3. Shock wave propagation under an above-critical load $f = 0.04$: displacement profiles: (a, b); fine scale temperature: (c, d); and coarse scale temperature: (e, f).

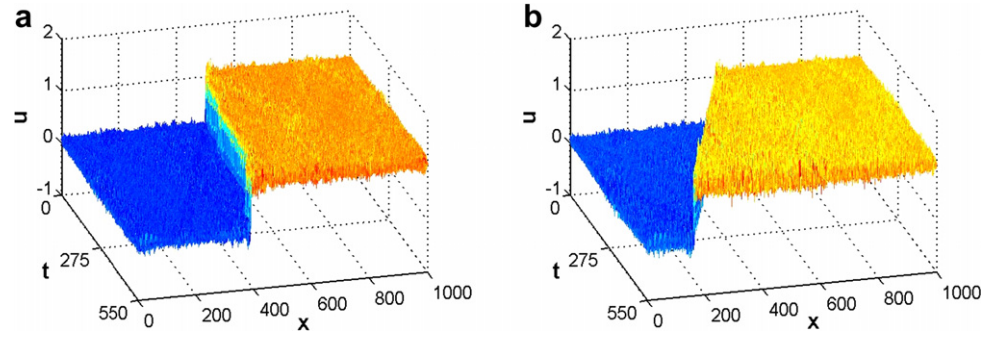

Fig. 4. Shock wave motion under a sub-critical load $f = 0.03$: (a) conventional NEMD simulation with initial temperature $T = 200$ K; (b) MS-NEMD simulation with initial temperature $T = 200$ K.

thermal fluctuation. For detailed information, readers are referred to the related full-length exposition [33].

In the third simulation, we compare the simulation results between the Nośe–Hoover equilibrium MD and MS-NEMD under the same initial temperature, $T_0 = 0$ K. For the equilibrium MD, its coarse scale or thermodynamic temperature will remain 0 K, whereas in the MS-NEMD simulation, the system's temperature will rise

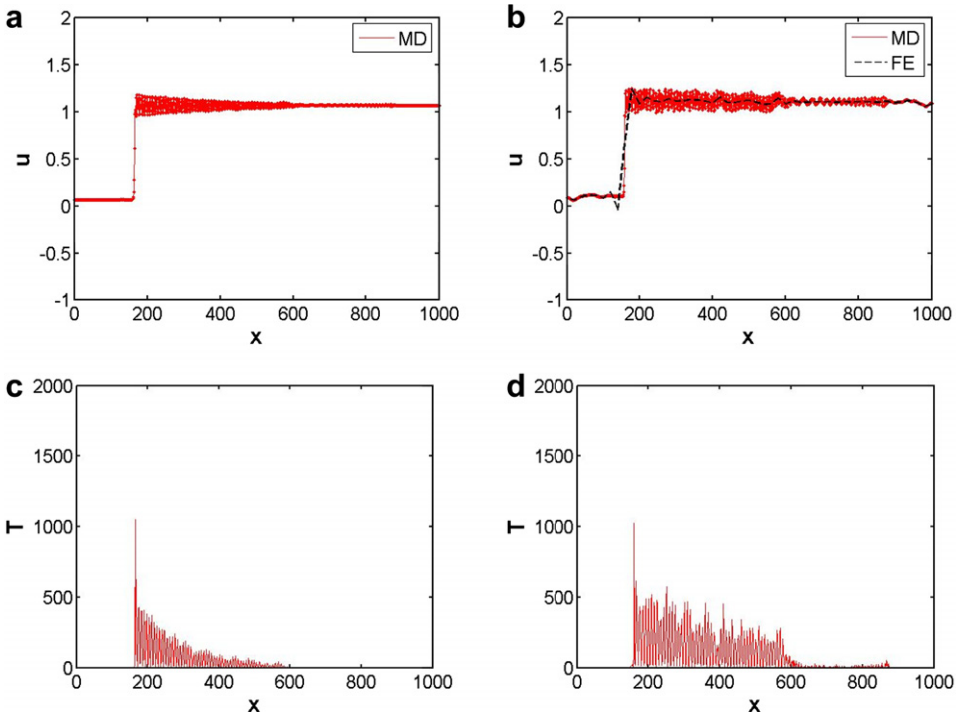

Fig. 5. Shock wave propagation: displacement profiles by (a) the Nośe–Hoover equilibrium MD and (b) MS-NEMD; instantaneous temperature profiles by (c) the Nośe–Hoover equilibrium MD and (d) MS-NEMD.

above to the initial temperature $T_0 = 0$ K, and its spatial distribution is non-uniform. In Fig. 5, we juxtapose both displacement profiles and *instantaneous temperature profiles* obtained from each method.

Since in the equilibrium MD simulations, the thermodynamic temperature is enforced at $T = 0$ K, subsequently it then puts the constraint on the kinetic energy distribution. Hence the instantaneous temperature distribution is visibly smaller than that of the MS-NEMD simulations. In other words, under the equilibrium state, the thermal–mechanical interaction is constrained, while under the non-equilibrium state, the thermal–mechanical interaction obeys the second law, and there will be thermal–mechanical energy conversion due to dissipations.

Recently, we have reported a multi-dimensional simulation by using MS-NEMD in [45], and it will be further discussed in the context of different atomic potentials in coming Letters.

Acknowledgement

This work is supported by a Grant from NSF (Grant No. CMS-0239130), which is greatly appreciated.

References

[1] S. Nosé, Mol. Phys. 52 (1984) 255.
[2] W.G. Hoover, Phys. Rev. A 31 (1985) 1695.
[3] S. Nosé, Mol. Phys. 57 (1986) 187.
[4] L.M. Hood, D.J. Evans, G.P. Morriss, Mol. Phys. 62 (1987) 419.
[5] H. Eslami, F. Müller-Plathe, J. Comput. Chem. 28 (2006) 1763.
[6] D.J. Evans, Phys. Rev. Lett. A 91 (1982) 457.
[7] F. Zhang, D.J. Isbister, D.J. Evans, Phys. Rev. E 61 (2000) 3541.
[8] M. Zhang, E. Lussetti, L.E.S. de Souza, F. Müller-Plathe, J. Phys. Chem. B 109 (2005) 15060.
[9] W.G. Hoover et al., Phys. Rev. A 22 (1980) 1690.
[10] D.J. Evans, G.P. Morriss, Phys. Rev. A 30 (1984) 1528.
[11] B.J. Edwards, C. Baig, D.J. Keffer, J. Chem. Phys. 123 (2005) 114106.
[12] B.L. Holian, P.S. Lomdahl, Science 280 (1998) 2085.
[13] W.G. Hoover, in: L. Garrido (Ed.), Systems Far from Equilibrium, Springer-Verlag, 1980, p. 373.
[14] D.J. Evans, G.P. Morriss, Statistical Mechanics of Nonequilibrium Liquids, Academic Press Inc., San Diego, 1990.
[15] M.E. Tuckerman, C.J. Mundy, S. Balasubramanian, M.L. Klein, JCP 106 (1997) 5616.
[16] M. Dressler, B.J. Edwards, Int. J. Mod. Phys. C 13 (2002) 1273.
[17] D.J. Evans, W.G. Hoover, B.H. Failor, B. Moran, A.J.C. Ladd, Phys. Rev. A 8 (1983) 1016.
[18] T.M. Galea, P. Attard, Phy. Rev. E 66 (2002) 041207.
[19] J.N. Bright, D.J. Evans, J. Chem. Phys. 122 (2005) 194106.
[20] A. Baranyai, Phys. Rev. E 54 (1996) 6911.
[21] F. Müller-Plathe, J. Chem. Phys. 106 (1997) 6082.
[22] S. Lepri, R. Livi, A. Politi, Phys. Rep. 377 (2003) 1.
[23] H.J. Castejon, J. Phys. Chem. B 107 (2003) 826.
[24] P. Chantrenne, J.-L. Barrat, ASME J. Heat Trans. 126 (2004) 577.
[25] F.F. Abraham, J. Broughton, N. Bernstein, E. Kaxiras, Europhys. Lett. 44 (1998) 783.
[26] R.E. Rudd, J.Q. Broughton, Phys. Rev. B 58 (1998) R5893.
[27] R.E. Rudd, J.Q. Broughton, Phys. Rev. B 72 (2005) 144104.
[28] G.J. Wagner, W.K. Liu, J. Comput. Phys. 190 (2003) 249.
[29] H.S. Park, E.G. Karpov, W.K. Liu, Int. J. Numer. Meth. Eng. 64 (2005) 237.
[30] W. E, Z. Huang, Phys. Rev. Lett. 87 (2001) 135501.
[31] W. E, B. Engquist, Z. Huang, Phys. Rev. B 67 (2003) 092101.
[32] R.E. Rudd, J.Q. Broughton, Phy. Rev. B 58 (1998) R5893.
[33] S. Li, N. Sheng, J. Chem. Phys. (submitted for publication).
[34] K. Kawasaki, D. Gunton, Phys. Rev. A 8 (1973) 2048.

[35] T. Taniguchi, G. Morriss, Phys. Rev. E 70 (2004) 056124.
[36] X. Liu, S. Li, J. Chem. Phys. 126 (2007) (Article No. 124105).
[37] T. Taniguchi, Physica A 236 (1997) 448.
[38] D.J. Diestler, Phys. Rev. B 66 (2002) 184104.
[39] H. Jiang, Y. Huang, K.C. Hwang, ASME J. Eng. Mater. Tech. 127 (2005) 408.
[40] J.H. Weiner, Statistical Mechanics of Elasticity, John Wiley & Sons, New York, 1983.
[41] T. Kontorova, Y.I. Frenkel, Zh. Eksp. Teor. Fiz. 8 (1938).
[42] R. Peierls, Proc. Phys. Soc. Lond. 52 (1940) 34.
[43] J. Hartford, B. von Sydow, G. Wahnstrom, B.I. Lundqvist, Phys. Rev. B 58 (1998) 2487.
[44] D.L. Olmsted, K.Y. Hardikar, R. Phillips, Model. Simul. Mater. Sci. Eng. 9 (2001) 215.
[45] N. Sheng, S. Li, Mech. Res. Commun. 34 (2007) (online).